Spatial correlations and cross sections of clusters in the $A+B\rightarrow 0$ reaction

R. Reigada,[1] F. Sagués,[1] I. M. Sokolov,[2,3] J. M. Sancho,[4] and A. Blumen[2]
[1]*Departament de Química Física, Universitat de Barcelona, Diagonal 647, Barcelona 08028, Spain*
[2]*Theoretische Polymerphysik, Universität Freiburg, Rheinstraße 12, D-79104 Freiburg im Breisgau, Germany*
[3]*P.N. Lebedev Physical Institute of the Academy of Sciences of Russia, Leninski Prospect 53, Moscow 117924, Russia*
[4]*Departament d'Estructura i Constituents de la Matèria, Universitat de Barcelona, Diagonal 647, Barcelona 08028, Spain*
(Received 6 September 1995)

We consider the distribution of cross sections of clusters and the density-density correlation functions for the $A+B\rightarrow 0$ reaction. We solve the reaction-diffusion equations numerically for random initial distributions of reactants. When both reactant species have the same diffusion coefficients the distribution of cross sections and the correlation functions scale with the diffusion length and obey superuniversal laws (independent of dimension). For different diffusion coefficients the correlation functions still scale, but the scaling functions depend on the dimension and on the diffusion coefficients. Furthermore, we display explicitly the peculiarities of the cluster-size distribution in one dimension.

PACS number(s): 05.40.+j, 82.20.−w, 82.40.−g

I. INTRODUCTION

Since the pioneering works by Ovchinnikov and Zeldovich [1] and Toussaint and Wilczek [2], much attention has been paid to the role of fluctuation effects on diffusion-controlled kinetics. In this context, the reaction $A+B\rightarrow 0$ was much investigated since it leads to nonclassical kinetic laws: Its kinetic regime is fluctuation dominated [3]; the concentration decay follows, for stoichiometrical conditions, the form $\rho\sim t^{-d/4}(d\leq 4)$ [3–6], whereas the classical kinetic law predicts $\rho\sim t^{-1}$.

The decay of the reactants' concentrations is thus slowed down; this is due to the formation of clusters (spatially segregated domains) of A and B particles during the course of the reaction [3,7–10], and to the fact that the reaction then takes place only at the clusters' boundaries. Much interest has thus focused on the spatial structure of the clusters and of their boundaries, and especially on scaling [7–12].

In the present work we concentrate on a precise characterization of the clusters through the determination of the density-density correlation functions and of the distributions of the clusters' cross sections. These quantities scale in general with respect to the diffusion length $\Lambda\tilde{}(Dt)^{1/2}$ [7-12]. We present results for all three spatial dimensions, both for equal and for unequal reactants' mobilities.

Our results are obtained from a usual, approximate system of reaction-diffusion equations for the local particles' densities. This approach allows effective numerical schemes and analytical insights. We are aware of the limitations of the approach, and this issue will be explicitly discussed when appropriate. Also see Ref. [13] for an in-depth analysis of this topic, and for a comparison of reaction-diffusion and of direct simulation results.

II. MODEL EQUATIONS AND NUMERICAL PROCEDURE

We model the reaction kinetics in terms of the usual reaction-diffusion equations (see, e.g., Ref. [9]) for the local densities $\rho_{A,B}$:

$$\frac{\partial\rho_A(\mathbf{r},t)}{\partial t}=D_A\Delta\rho_A(\mathbf{r},t)-k\rho_A(\mathbf{r},t)\rho_B(\mathbf{r},t) \tag{1}$$

and

$$\frac{\partial\rho_B(\mathbf{r},t)}{\partial t}=D_B\Delta\rho_B(\mathbf{r},t)-\rho_A(\mathbf{r},t)\rho_B(\mathbf{r},t)\ . \tag{2}$$

Here k is a time-independent rate coefficient, and D_A and D_B are the diffusion coefficients of the reactants. We note that the deterministic reaction-diffusion Eqs. (1) and (2) reproduce the kinetics fairly well. Quantitatively, however, care must be exercised; see Ref. [13] for a detailed discussion.

When $D_A=D_B$ holds, the system described by Eqs. (1) and (2) can be explored to a large extent analytically. This is due to the prevailing high symmetry of the problem. For $D_A\neq D_B$ we obtain most of the results numerically.

We solve the coupled partial differential equations (PDE's), Eqs. (1) and (2), by using a standard discrete scheme with a centered form for the Laplacian operator with periodic boundary conditions and a forward difference in time (see e.g., [14]). In higher dimensions the handling of the numerical code is largely improved by vectorizing the corresponding lattices into a one-dimensional (1D) array. The initial particle distribution is taken to be Poissonian, with equal mean for both species: $\rho_A(t=0)=\rho_B(t=0)=1.0$. The situation is stoichiometric, and thus $\langle\rho_A(\mathbf{r},t)\rangle=\rho_A(t)=\rho_B(t)=\langle\rho_B(\mathbf{r},t)\rangle$, where the average is taken over all sites $\mathbf{r}$. In the following we set $\rho(t)\equiv\rho_A(t)=\rho_B(t)$. We take simple cubic lattices of sidelength $L=10\,000$ in $d=1$, $L=150$ in $d=2$, and $L=50$ in $d=3$. We discretize time and space in increments of $\Delta t=0.01$ and $\Delta x=1$. This choice guarantees that the scheme is numerically stable and convergent for the values of ρ, k, and $D_{A,B}$ used here. We take care to avoid finite-size effects by never letting the linear mean cluster size exceed 0.2 L. Then k and D have to be chosen judiciously in order to detect

 ©1996 The American Physical Society

clustering within reasonable computer times. In all what follows we took $k=10$ and fixed the value of $D=(D_A+D_B)/2$ to $D=1$ for $d=1$, $D=0.1$ for $d=2$, and $D=0.01$ for $d=3$. The individual diffusion coefficients were varied, and included the analytically tractable case $D_A=D_B$ as well as the extreme case $D_B=0$. All calculations were performed on the CRAY Y-MP/232 of Centre de Supercomputació de Catacunya.

III. DECAY PATTERNS

For the sake of completeness, in Fig. 1 we present $\rho(t)$ for several (D_A,D_B) values for $d=1$, 2, and 3. The results are obtained from ten different realizations of the initial conditions, and are plotted in double-logarithmic scales. In Fig. 1 one recognizes readily the asymptotic kinetics, $\rho\sim t^{-d/4}(d\leq 4)$. We obtain this regime, regardless of the specific D_B/D_A ratio, in all three dimensions. This reproduces the findings of Refs. [4,13,15]. The asymptotic domain is reached earlier when one of the reactive species becomes less mobile, i.e., when D_A and D_B differ very much. This is not all surprising, since in the context of diffusion-limited reactions, clusters are the signature of a poor mixing efficiency.

IV. SPATIAL CORRELATIONS AND CLUSTER STATISTICS

Here we analyze the clusters emerging during the reaction in terms of correlation functions and cluster cross-section distributions. A standard way is to use density-density correlation functions. For particles of the same kind we have

$$C_{AA}(\mathbf{r}')=\frac{\langle\rho_A(\mathbf{r})\rho_A(\mathbf{r}+\mathbf{r}')\rangle}{\langle\rho_A(\mathbf{r})\rangle^2} \tag{3}$$

and similarly for $C_{BB}(\mathbf{r}')$. For particles of different kinds we have

$$C_{AB}(\mathbf{r}')=\frac{\langle\rho_A(\mathbf{r})\rho_B(\mathbf{r}+\mathbf{r}')\rangle}{\langle\rho_A(\mathbf{r})\rangle\langle\rho_B(\mathbf{r})\rangle} . \tag{4}$$

Furthermore, clusters are easily defined in terms of the densities of the particles. For this, consider the function $\gamma(\mathbf{r},t)\equiv\rho_A(\mathbf{r},t)-\rho_B(\mathbf{r},t)$, which vanishes at the boundaries of the clusters. Hence it is sufficient to determine the zeros of $\gamma(\mathbf{r},t)$ in order to have the cluster structure; e.g., for $d\neq 1$ we obtain the distribution of cross sections from the zeros of $\gamma(\mathbf{r},t)$ along arbitrary straight lines drawn through the system. In $d=1$ we take 100 realizations of initial particle distributions. In $d=2$ and 3 we use some 50 realizations. For each realization and at each needed time we determine the zeros of $\gamma(\mathbf{r},t)$ along 50 random straight lines drawn parallel to the coordinate axis.

We now turn to the presentation of our results, and consider the cases $D_A=D_B$ and $D_A\neq D_B$ separately.

A. Case $D_A=D_B$

We start in Fig. 2 by presenting the correlation functions $C_{AA}(\mathbf{r})$ and $C_{AB}(\mathbf{r})$. The results are computed at different times, and averaged over 100 different initial distributions. The plots are given as a function of the scaling variable $r/(Dt)^{1/2}$. Note that results for different times and different dimensions fall on the same (master) curve, an indication of superuniversal behavior. We show, following Ref. [15], that the reason for this is the fact that $D_A=D_B$, which renders $\gamma(\mathbf{r},t)$ Gaussian in space. From Eqs. (1) and (2) it follows that for $D_A=D_B\equiv D$ $\gamma(\mathbf{r},t)$ obeys the exact diffusion equation

$$\frac{\partial\gamma(\mathbf{r},t)}{\partial t}=D\Delta\gamma(\mathbf{r},t) . \tag{5}$$

Note that for $D_A\neq D_B$ Eq. (5) does not hold; it is replaced by a *nonlinear* diffusion equation; see Ref. [13]. The formal solution of Eq. (5) reads

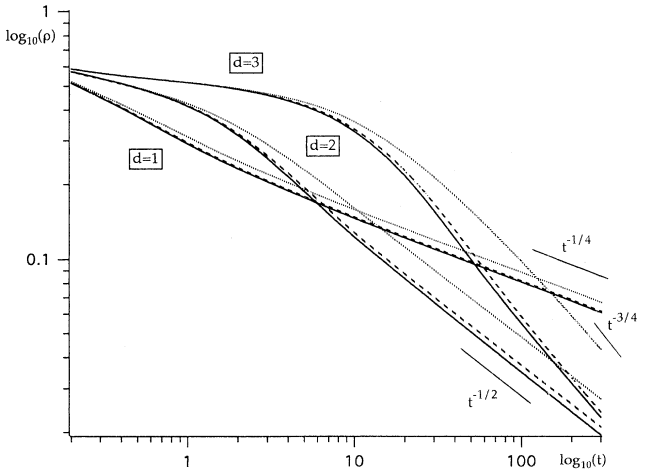

FIG. 1. Particle densities as a function of time for different dimensions and different D_B/D_A ratios: 0 (dotted lines), $\frac{1}{3}$ (dashed lines), and 1 (solid lines). Note the double logarithmic scales. See text for details.

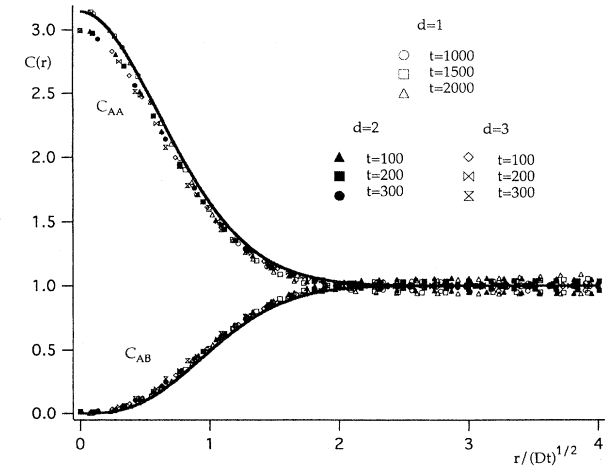

FIG. 2. Density-density correlation functions C_{AA} and C_{BB} for $D_A=D_B$, plotted as a function of $r/(Dt)^{1/2}$. The full lines are the analytical Eqs. (15) and (16). Note the dimension independence (superuniversality) of the results.

$$\gamma(\mathbf{r},t)=\int_{-\infty}^{\infty}\gamma(\mathbf{r}',0)G(\mathbf{r}-\mathbf{r}',t)dt\ , \tag{6}$$

where $G(\mathbf{r},t)=(4\pi Dt)^{-d/2}\exp(-\mathbf{r}^2/4Dt)$ is the Green's function of Eq. (5). From Eq. (6) it follows that $\gamma(\mathbf{r},t)$ is a weighted sum of the initial $\gamma(\mathbf{r},0)$ values, which are uncorrelated. Hence $\gamma(\mathbf{r},t)$ is a Gaussian random process *in space*. This process is fully characterized by its mean (which in our case vanishes) and its two-point correlation function $R_t(\mathbf{x}_1,\mathbf{x}_2)$. The correlation function is

$$R_t(\mathbf{x}_1,\mathbf{x}_2)=\int\int G(\mathbf{x}_1-\mathbf{x}',t)G(\mathbf{x}_2-\mathbf{x}'',t)\times c(\mathbf{x}',\mathbf{x}'')d\mathbf{x}'d\mathbf{x}''\ , \tag{7}$$

where $c(\mathbf{x},\mathbf{y})$ is the correlation function of the γ for $t=0$, Ref. [15]:

$$c(\mathbf{x},\mathbf{y})=\langle\gamma(\mathbf{x},0)\gamma(\mathbf{y},0)\rangle=2\rho(0)\delta(\mathbf{x}-\mathbf{y})\ . \tag{8}$$

The evaluation of Eq. (7), together with Eq. (8) then gives

$$R_t(r)=2\rho(0)(8\pi Dt)^{-d/2}\exp(-r^2/8Dt)\ , \tag{9}$$

with $r=|\mathbf{x}_1-\mathbf{x}_2|$.

In the diffusion-limited case, for $k\to\infty$, the cluster boundaries are very narrow. Evidently, to a very good approximation one then has:

$$\rho_A(\mathbf{x},t)=\gamma(\mathbf{x},t)\Theta(\gamma(\mathbf{x},t)) \tag{10}$$

and

$$\rho_B(\mathbf{x},t)=-\gamma(\mathbf{x},t)\Theta(-\gamma(\mathbf{x},t))\ , \tag{11}$$

where $\Theta(x)$ is the Heaviside theta function. From these expressions the correlation functions Eqs. (3) and (4) follow [16]:

$$\langle\rho_A(\mathbf{x},t)\rho_X(\mathbf{x}+\mathbf{r},t)\rangle=\int_0^{\infty}\int_{-\infty}^{\infty}\gamma_1\gamma_2\Theta(\pm\gamma_2)P(\gamma_1,\gamma_2;\mathbf{r})d\gamma_1 d\gamma_2\ . \tag{12}$$

In Eq. (12) the sign is positive for $X=A$ and negative for $X=B$. Moreover,

$$p(\gamma_1,\gamma_2;\mathbf{r})=\frac{1}{2\pi R_t(0)\sqrt{1-g^2}}\exp\left[-\frac{\gamma_1^2+\gamma_2^2-2\gamma_1\gamma_2 g}{2R_t(0)(1-g^2)}\right] \tag{13}$$

is the two-point joint probability density for γ, with

$$g(\mathbf{r},t)=R_t(\mathbf{r})/R_t(0)=\exp(-\mathbf{r}^2/8Dt)\ . \tag{14}$$

The evaluation of the integrals in Eq. (12) now readily gives

$$C_{AA}=(1-g^2)^{3/2}+g^2(1-g^2)^{1/2}-g\arctan\left[\frac{(1-g^2)^{1/2}}{g}\right]+\pi g \tag{15}$$

and

$$C_{AB}=(1-g^2)^{3/2}+g^2(1-g^2)^{1/2}-g\arctan\left[\frac{(1-g^2)^{1/2}}{g}\right]\ . \tag{16}$$

The analytical expressions Eqs. (15) and (16) are also plotted in Fig. 2. The agreement is very good, especially when realizing that the analytical results hold in the $k\to\infty$ limit. We note that Eqs. (15) and (16) were also checked in 1D with the help of direct simulations, in which the A and B particles perform random walks and react on contact; the procedure is identical to the one reported in Ref. [17] for interacting particles.

We turn now to the cross sections of clusters. The cross sections are given by the segments of straight lines inside cluster boundaries. We denote by $p(s,t)$ the distribution of such cross sections at time t. Note that in 1D this distribution coincides with the cluster size distribution. It was obtained in Ref. [18] for a layered system, but as we show in the following, the result is valid in general, provided that $D_A=D_B$.

For $d=2$ and 3 we have drawn lines parallel to the coordinate axes. Evidently, the problem considered here is isotropic. Theoretically, the difference variable $\gamma(x,t)$ considered as a function of the coordinate along this line is a one-dimensional Gaussian random process. The cluster boundaries then correspond to simple zeros of the Gaussian process, whose statistics are well known and can be expressed through the joint probability distribution of $\gamma(x,t)$ and its spatial derivatives. The calculations are given explicitly in Ref. [18]. Here we summarize the results.

The cluster cross-section distribution $p(s,t)$ can be expressed in terms of a function $g(x,t)$, Eq. (14), and therefore depends on cross-section length s and time t only through a scaling variable $\zeta=s/(8Dt)^{1/2}$.

The scaled distribution density $p(\zeta)$ [defined as $p(s,t)(Dt)^{1/2}$] can be obtained from the conditional probability $P(\zeta|0)$ to find a cluster boundary at ζ, provided there is one at 0. The relation is of Ornstein-Zernike type:

$$P(\zeta|0)=p(\zeta)+\int_0^{\zeta}p(\xi)P(\xi-\zeta|0)d\xi\ . \tag{17}$$

Equation (17) can be readily evaluated numerically. $P(\zeta|0)$ is given by [18]

$$P(\zeta|0)=\frac{(\mu_{33}^2-\mu_{34}^2)^{1/2}}{\pi^2[1-g^2(\zeta)]^{3/2}}\left[1+\frac{\mu_{34}}{(\mu_{33}^2-\mu_{34}^2)^{1/2}}\arctan\frac{\mu_{34}}{(\mu_{33}^2-\mu_{34}^2)^{1/2}}\right] \tag{18}$$

written in terms of the functions

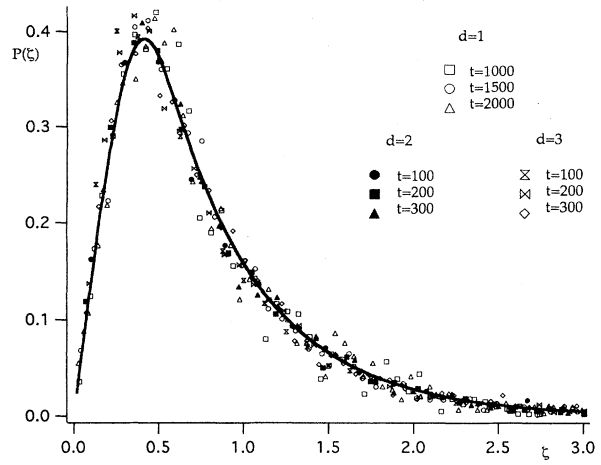

FIG. 3. Cross-section length distributions for $D_A=D_B$ as a function of $\zeta=x/(8Dt)^{1/2}$. The solid line represents the analytical results, Eqs. (16)–(19). Note the superuniversality of the rescaled distribution.

$$\mu_{33}=g''(0)[1-g^2(\zeta)]+g'^2(\zeta) \tag{19}$$

and

$$\mu_{34}=g''(\zeta)[1-g^2(\zeta)]+g'^2(\zeta)g(\zeta)\ , \tag{20}$$

with $g(\zeta)=\exp(-\zeta^2)$, Eq. (14).

Results from our numerical simulations together with the analytical scaling curve are plotted in Fig. 3. Note that the cross-section distributions obtained here for $d=2$ and 3 mimic the behavior found in $1D$; see also simulations of Ref. [12]: $p(\zeta)$ increases linearly for small ζ and decays exponentially for large ζ.

B. Case $D_A \neq D_B$

Without loss of generality we take $D_A > D_B$. Figure 4 shows in scaling form the correlation function in $d=2$ for $D_B=0$. For $0<D_B<D_A$ the results are qualitatively similar to $D_B=0$, apart from the fact that C_{BB} stays finite at $r=0$. We summarize our findings as follows:

(i) All correlations functions scale with $t^{1/2}$.

(ii) C_{AA} and C_{BB} depend strongly on D_A and D_B. For $D_B=0$, C_{BB} is very large for small Λ; furthermore, for small Λ C_{AA} is smaller than C_{BB}. This is a reflection of the fact that now large (and sparsely populated) A domains are randomly "drilled" by small (but densely populated) B domains; the later retain their initial, Poisson distribution.

(iii) We were not able to find any universal scaling for the correlation functions. Their form depends on details, such as the particular D_A, D_B values and on the dimension.

Now we turn to the distribution of cluster cross sections for $D_A > D_B$. The results for $D_B \neq 0$ are qualitatively similar to those for $D_A=D_B$: both $p_A(s,t)$ and $p_B(s,t)$ scale with $\zeta=s/(8Dt)^{1/2}$, but now show different forms, which depend on D_A and D_B. On the other hand, the results for $D_B=0$ are very special.

In Fig. 5(a) we present for $D_B=0$ the cross-section dis-

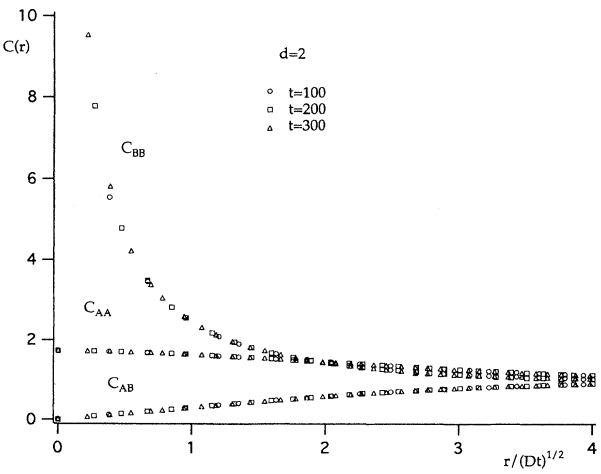

FIG. 4. Density-density correlation functions as a function of $r/(Dt)^{1/2}$ for $D_B=0$ in $d=2$.

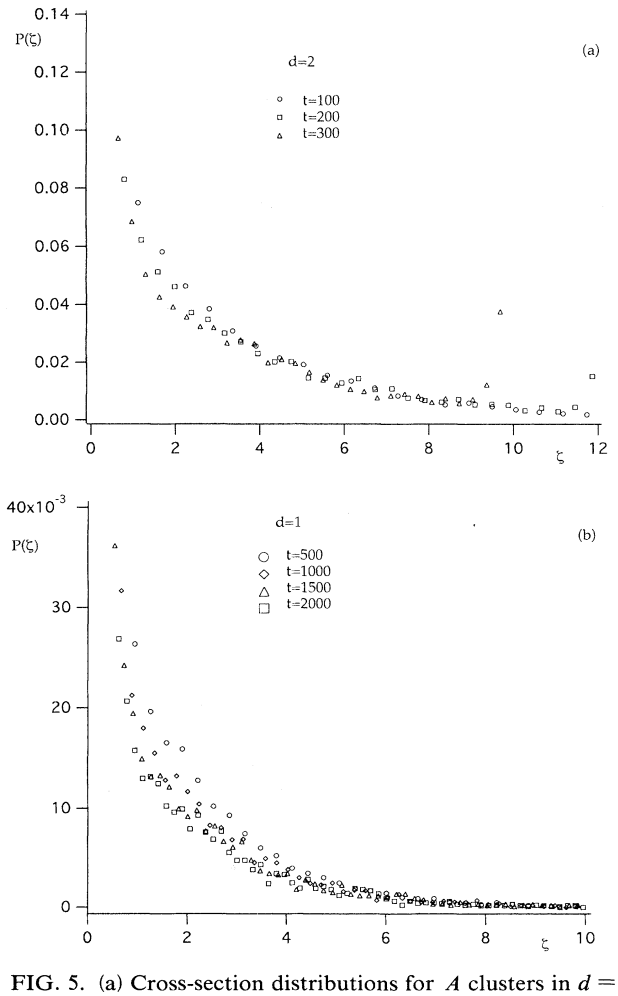

FIG. 5. (a) Cross-section distributions for A clusters in $d=2$ for $D_B=0$. (b) The same as in (a), now in $d=1$. Note that at small distances the functions do not scale.

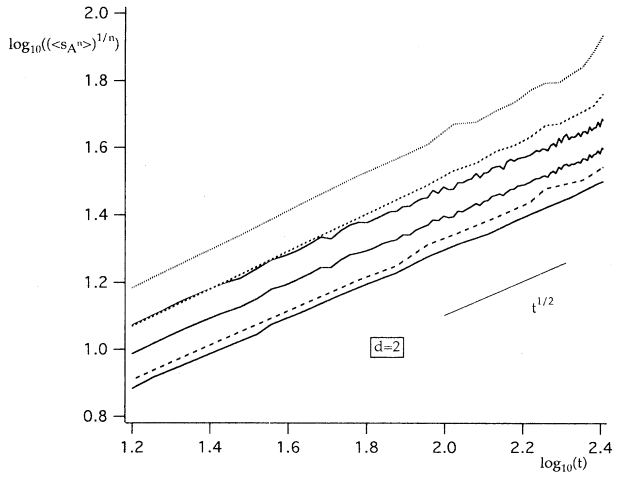

FIG. 6. The first three reduced moments $\langle s_A^n(t)\rangle^{1/n}$ in $d=2$. The solid lines correspond to $D_A=D_B$, the broken ones to the case $D_B=0$.

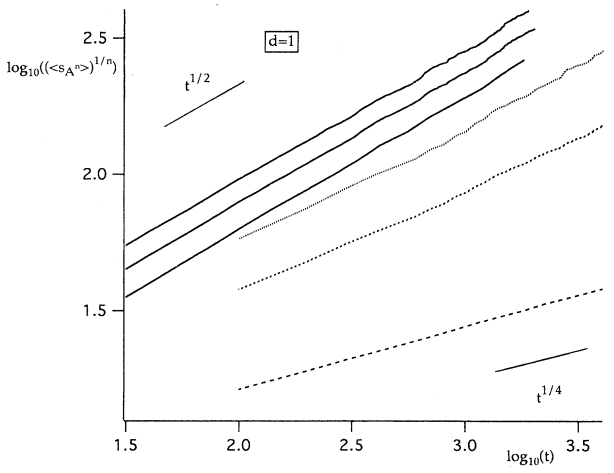

FIG. 7. Same as in Fig. 6, now in $d=1$. Note the lack of scaling for $D_B=0$.

tribution for the A species in $d=2$, and in Fig. 5(b) that in $d=1$. For the sake of easy comparison to Fig. 3, we rescaled the results as a function of ξ. The situation in $d=3$ is qualitatively similar to the $d=2$ case, and we refrain from presenting it here.

In view of the results of Figs. 5 for $D_B=0$, scaling is less conclusive than for $D_A=D_B$. The distribution $p_A(s,t)$ seems to scale for large, but not for small, ξ. To gain a better understanding of the scaling properties of the cross-section distributions, we now focus on the reduced moments $\langle s_A^n(t)\rangle^{1/n}$. If all moments obey the usual diffusive pattern, one finds $\langle s_A^n(t)\rangle^{1/n}\sim t^{1/2}$ for all n. In Fig. 6 we present the first three moments ($n=1$, 2, and 3) for $d=2$ and in Fig. 7 those for $d=1$. The results were obtained from 50 different initial realizations in $d=2$ and 3. In $d=1$ we again take 100 realizations directly.

For $D_A=D_B$ all three moments scale with $t^{1/2}$ both in $d=1$ and in $d=2$. For $D_B=0$ our conclusions are as follows.

(i) For $d=2$ scaling practically obeys t^{α}, with α being the same for $n=1$, 2, and 3, and being only slightly different from $\frac{1}{2}$. The difference may even be due to finite-size effects or to higher-order corrections to scaling. The same holds for $d=3$.

(ii) In $d=1$ the situation is singular. We now have $\langle S_A^n(t)\rangle^{1/n}\sim t^{\alpha_n}$, where the exponents α_n increase with n, possibly tending to $\frac{1}{2}$; this may indicate that only the largest clusters grow diffusively. This finding, and the fact that C_{BB} seems to depend little on time, contrasts with the result of Ref. [12], which reports scaling with $(Dt)^{1/2}$.

A careful analysis shows the reason for this peculiar behavior in $d=1$. In a continuous picture an A cluster can either coalesce with a neighboring one if the B wall between them is thin enough to be eaten away or it persists indefinitely, if its neighboring B walls are very thick. In the last case the particle concentration inside the A cluster decreases with time but does not reach zero at a finite time. These small clusters form the nonscaling small-size background seen in Fig. 5(b). Conversely, in a discrete particle picture, small A clusters disappear: When all the A particles between two B walls have reacted, the A cluster ceases to exist. The neighboring B clusters coalesce, a mechanism which gives rise to B-cluster growth and to scaling behavior for both $p_A(s,t)$ and $p_B(s,t)$, as also found in Ref. [12].

Note that small A clusters with exponentially low concentrations can influence neither the kinetic behavior nor the density-density correlation functions; they show up, however, in considerations of the cluster-size distributions, where they significantly change the normalization constant.

This finding shows that the geometrical properties of clusters may depend sensitively on the underlying microscopic model; thus continuum models in $d=1$ give rise to nonuniversal behavior. This nonuniversality may be either an artifact (if it is only a mesoscopic approximation for a discrete system) or a physical effect, say in a system with initial macroscopic inhomogeneities (e.g., a layered system; see Ref. [19]).

V. CONCLUSIONS

Here we analyzed statistical properties of clusters formed during the $A+B\rightarrow 0$ reaction. The clusters are characterized by the density-density correlation functions and by their cross-section distributions. We have found that, for equal diffusion coefficients $D_A=D_B$, the behavior of both quantities is superuniversal (independent of dimension); it is governed only by the diffusion length $\Lambda\sim(Dt)^{1/2}$. When $D_A\neq D_B$ the correlation functions scale, but their explicit forms depends on d and on D_A and D_B. For $D_B=0$ and $d=1$ no scaling is evident in the cross-section distribution.

ACKNOWLEDGMENTS

The support of the DFG through the SFB 60 and of the Fonds der Chemischen Industrie is gratefully acknowledged. This research was jointly supported by Direccion General de Investigacion Cientifica y Tecnologica (DGICYT) Spain under Project Nos PB93-759 and PB93-769, and the Comissionat per Universitats i Recerca de la Generalitat de Catalunya. R.R. benefitted from a FI grant from Generalitat de Catalunya. F.S. Benefitted from a BE/AI grant from Direccio General de Recerca.

[1] A. A. Ovchinnikov and Ya. B. Zeldovich, Chem. Phys. **28**, 215 (1978).
[2] D. Toussaint and F. Wilczsek, J. Chem. Phys. **78**, 2642 (1983).
[3] K. Kang and S. Redner, Phys. Rev. Lett. **52**, 955 (1984).
[4] K. Kang and S. Redner, Phys. Rev. A **32**, 435 (1985).
[5] P. Meakin and H. E. Stanley, J. Phys. A **17**, L173 (1984).
[6] V. N. Kuzovkov and E. A. Kotomin, Rep. Prog. Phys. **51**, 1479 (1988).
[7] I. M. Sokolov, Pis'ma Zh. Eksp. Teor. Fiz. **44**, 53 (1986) [JETP Lett. **44**, 67 (1986)].
[8] L. A. Harmon, L. Li, L. W. Anacker, and R. Kopelman, Chem. Phys. Lett. **163**, 463 (1989).
[9] P. Argyrakis, R. Kopelman, and K. Lindenberg, Chem. Phys. **177**, 693 (1993).
[10] F. Leyvraz and S. Redner, Phys. Rev. Lett. **66**, 2168 (1991).
[11] B. P. Lee and J. Cardy, Phys. Rev. E **50**, R3287 (1994).
[12] F. Leyvraz and S. Redner, Phys. Rev. A **46**, 3132 (1992).
[13] G. Zumofen, J. Klafter, and A. Blumen, Phys. Rev. A **44**, 8390 (1991).
[14] S. E. Koonin and D. C. Meredith, *Computational Physics* (Addison-Wesley, Reading, MA, 1990).
[15] I. M. Sokolov, H. Schñorer, and A. Blumen, Phys. Rev. A **44**, 2388 (1991).
[16] A. G. Vitukhnovsky, B. L. Pyttel, and I. M. Sokolov, Phys. Lett. A **128**, 161 (1988).
[17] I. M. Sokolov, P. Argyrakis, and A. Blumen, J. Phys. Chem. **98**, 7256 (1994).
[18] I. M. Sokolov, and A. Blumen, Phys. Rev. A **43**, 6545 (1991).
[19] I. M. Sokolov and A. Blumen, Int. J. Mod. Phys. B **5**, 3127 (1991).